Crystal Structure, Magnetic Order, and Vibrational Behavior in Iron Rare-Earth Borates

J. A. Campá,[1a] C. Cascales,[1b] E. Gutiérrez-Puebla,[1b] M. A. Monge,[1b] I. Rasines,*[,1b] and C. Ruíz-Valero[1b]

Facultad de Ciencias Geológicas, Universidad Complutense de Madrid, 28040 Madrid, and Instituto de Ciencia de Materiales, CSIC, Cantoblanco, 28049 Madrid, Spain

Received May 31, 1996. Revised Manuscript Received September 18, 1996[⊗]

Crystals of $Fe_3R(BO_3)_4$ (R = Y, La, Nd) have been grown. Their structure and properties show close relations. The structures of these materials have been established by single-crystal X-ray diffraction. They crystallize in the huntite, $CaMg_3(CO_3)_4$, structure type, trigonal system, space group *R*32 (No. 155), $Z = 3$, with unit-cell parameters (Å) $a = 9.592(1)$, 9.578(1), and 9.563(2) and $c = 7.597(7)$, 7.605(3), and 7.575(2), for R = La, Nd, and $Y_{0.5}Bi_{0.5}$, respectively. They contain RO_6 trigonal prisms and smaller FeO_6 octahedra forming layers and giving rise to Fe−R distances of ≃3.78 Å. RO_6 polyhedra are interconnected within the layers by corner sharing with triangular BO_3 groups of two types and FeO_6 octahedra. FeO_6 octahedra form 1D helicoidal chains with relatively short Fe−Fe distances, ≃3.18 Å. The temperature dependence of the magnetic susceptibility from 350 to 1.8 K for $Fe_3R(BO_3)_4$ shows two maxima at about 260 and 35 K and, for R = Nd, another maximum at 6 K. The presence of magnetic order is attributed to magnetic Fe−Fe or Fe−O−Fe interactions. Infrared spectra in the range 4000−240 cm^{-1} show the ν_1, ν_3, and ν_4 IR-active bands of the $B(1)O_3^{3-}$ triangular groups as well as ν_2 of less symmetrical $B(2)O_3^{3-}$.

Introduction

A good number of transparent rare-earth borates of composition $M_3R(BO_3)_4$ (M = Al, Ga, Cr, Fe, Sc; R = Y, La−Lu) are known as materials that integrate in one crystalline matrix two optical features, lasing and second harmonic generation.[2] These materials have been found to be isostructural with the mineral huntite, $CaMg_3(CO_3)_4$, whose crystal structure has been established and refined[3] from X-ray powder diffraction data in the trigonal space group *R*32.

The $Fe_3R(BO_3)_4$ family was first[4] prepared in polycrystalline form. Some of these borates (R = Y, Nd, Sm, Gd, Dy, Ho) are known to be paramagnetic[4] from 78 to 730 K. Although crystals of $Fe_3R(BO_3)_4$ (R = Y, La, Nd, Gd, Er) have been grown,[5,6] their crystal structure was not established from single-crystal X-ray diffraction data. Since interesting relations can be found between crystal structure and properties of materials containing **d** and **f** cations embedded in a matrix of **p** elements, here we present the crystal-structure refinement, the results of magnetic measurements from 350 to 1.8 K, and the characterization by infrared spectroscopy of three of these compounds (R = Y, La, Nd).

Experimental Section

Crystal Growth. $Fe_3R(BO_3)_4$ (R = Y, La, Nd) crystals were grown using Bi_2O_3 as a flux in platinum crucibles from reagent-grade mixtures of Fe_2O_3, R_2O_3, and B_2O_3 at molar ratios Fe:R:B:Bi = 1:0.5:2:5. These mixtures were heated in an electric furnace to 1000 °C, soaked for 1 h, cooled to 700 °C at 3 and 1 °C h^{-1} and to room temperature by turning the power off. After removing the flux with nitric acid, paper filtration allowed to recover the crystals, which were characterized by energy-dispersive X-ray analysis and X-ray powder diffraction as indicated elsewhere.[7]

X-ray Structure Determinations. The structure of $Fe_3R(BO_3)_4$ (R = Y, La, Nd) was determined by single-crystal X-ray diffraction methods. Transparent crystals showing well-defined faces were mounted in a Nonius CAD-4 diffractometer. The cell dimensions were refined by least-squares fitting the θ values of 25 reflections, resulting hexagonal parameters of isostructural compounds. A summary of the fundamental crystal and refinement data are given in Table 1. The systematic absence $-h + k + l = 3n + 1$ is consistent with trigonal space groups $R\bar{3}m$, $R3m$, $R32$. Intensity data were collected in the $\omega/2\theta$ scanning mode with standard reflections monitored for intensity changes throughout the data collections. The intensities were corrected for Lorentz and polarization effects. Scattering factors for neutral atoms and anomalous dispersion corrections for Y, La, Nd, Bi, and Fe were taken from the *International Tables for X-Ray Crystallography*.[8] The atomic coordinates[3] from the huntite mineral were taken as the starting point for the refinement. The small *R* factors obtained from the structure resolution confirmed the space group *R*32. In the Y compound the isotropic thermal parameters for the Y atom had a negative value, and it was necessary to refine its occupancy factor. The energy-dispersive X-ray analysis had shown that the Y crystal contained a fair amount of Bi from the flux and effectively the site (3a) was found to be occupied by Y and Bi with a population factor for Bi of 0.50(6). After refining the occupancy of the Y atom, the isotropic thermal parameter changed to a normal and positive value and the *R* value was lower. An empirical absorption

[⊗] Abstract published in *Advance ACS Abstracts,* November 15, 1996.

(1) (a) Universidad Complutense. (b) Instituto de Ciencia de Materiales.
(2) Keszler, D. A. *Curr. Opin. Solid State Mater. Sci.* **1996**, *1*, 204.
(3) Dollase, W. A.; Reeder, R. J. *Am. Mineral.* **1986**, *71*, 163.
(4) Joubert, J.-C.; White, W. B.; Roy, R. *J. Appl. Cryst.* **1968**, *1*, 318.
(5) Takahashi, T.; Yamada, O.; Ametani, K. *Mater. Res. Bull.* **1975**, *10*, 153.
(6) Maltseva, L. I.; Leonyuk, N. I.; Timchenko, T. I. *Krist. Tech.* **1980**, *15*, 35.
(7) Campá, J. A.; Gutiérrez Puebla, E.; Monge, M. A.; Rasines, I.; Ruíz Valero, C. *J. Cryst. Growth* **1992**, *125*, 17.
(8) Cromer, D. T.; Waber, J. T. In *International Tables for X-Ray Crystallography*; Ibers, J. I., Hamilton, W. C., Eds.; Kynoch Press: Birmingham, 1974; Vol. IV, pp 78, 81, 87, 88, 94.

S0897-4756(96)00313-4 CCC: $14.00

Table 1. Crystal and Refinement Data for $RFe_3(BO_3)_4$

crystal system	trigonal		
space group	*R*32 (No. 155)		
Z	3		
temp, K	295		
diffractometer	Enraf-Nonius		
radiation	graphite-monochromated Mo Kα (λ = 0.710 69 Å)		
2θ range, deg	2−60		
scan technique	$\omega/2\theta$		
data collected	(0,0,0) to (13,13,10)		
standard reflections	3/24		
R	La	Nd	$Y_{0.5}Bi_{0.5}$
mol wt	541.7	547.0	551.6
cell dimensions			
a, Å	9.592(1)	9.578(1)	9.563(2)
c, Å	7.597(7)	7.605(3)	7.575(2)
V, Å^3	605(4)	604(2)	600(2)
D_{calc}, g cm^{-3}	4.5	4.5	4.6
F(000)	753	762	765
μ(Mo Kα), cm^{-1}	105.8	117.5	199.7
crystal dimensions, mm	0.1 × 0.1 × 0.1	0.25 × 0.1 × 0.1	0.1 × 0.1 × 0.3
total no. of data	744	741	744
obsd reflections	234	234	230
R_{int} (%)	1.1	4.1	3.4
weighting scheme	file	file	unit
$R = \sum\|\Delta F\|/\sum\|F_o\|$	2.3	2.2	2.9
$R_w = (\sum w\Delta^2 F/\sum w\|F_o\|^2)^{1/2}$	1.1	2.3	3.4
max shift/error	0.015	0.005	0.04
absorption correction range	0.92−1−12	0.98−1.0	0.99−1.0

correction[9] was applied at the end of the isotropic refinements. For R = Y a final anisotropic full matrix least-squares refinement was undertaken with unit weights. No trend in *F* vs F_o or sin θ/λ was observed. For R = La, Nd the last steps of the refinement were calculated by PESOS[10] with weights $w = w_1w_2$, where $w_1 = 1/(a + b|F_o|)^2$, $w_2 = 1/(c + d(\sin\theta/\lambda))$. Final difference synthesis showed no significant electron density. Most of the calculations were carried out with the X-Ray 80 System.[11]

Magnetic Measurements. Dc magnetic measurements were carried out using a SQUID (Quantum Design) magnetometer operating from 350 to 1.8 K at 1000 (R = La, Nd) or 5000 Oe (R = Y). Diamagnetic corrections[12] for magnetic susceptibilities were introduced.

Spectroscopic Study. A FT-IR Nicolet SX60 spectrometer was used in the range 4000−240 cm^{-1} with powdered crystals dispersed in KBr.

Results and Discussion

$Fe_3R(BO_3)_4$ crystals were transparent, light yellow (R = Y), dark olive green (R = La) or bluish black (R = Nd), and showed forms of hexagonal prisms elongated along the *c* axis (Figures 1 and 2) and combined with either basal pinacoids (Figure 1), or negative $(2\bar{1}\bar{1}1)$ rhombohedra (Figure 2). Cooling rates of 3 and 1 °C h^{-1} led to crystal sizes of 1 and 3 mm, respectively.

Atomic position coordinates and isotropic thermal parameters as well as the main interatomic distances and angles for $Fe_3R(BO_3)_4$ (R = Y, La, Nd) are included in Tables 2 and 3. In these compounds three kinds of coordinations with oxygen are present: distorted RO_6 trigonal prisms, smaller FeO_6 octahedra, and two types of triangular BO_3 groups. The 12 borate anions in the unit cell of the $Fe_3R(BO_3)_4$ structure are found to divide into two sets. In the larger set at the (9e) position there are nine $B(2)O_3$ borates, which are isosceles triangles with its 2-fold rotation axis parallel to the *ab* crystal plane. In the smaller set each of the three borate anions, with B(1) at (3b) position, is a regular triangle and has its 3-fold rotation axis orientated parallel to

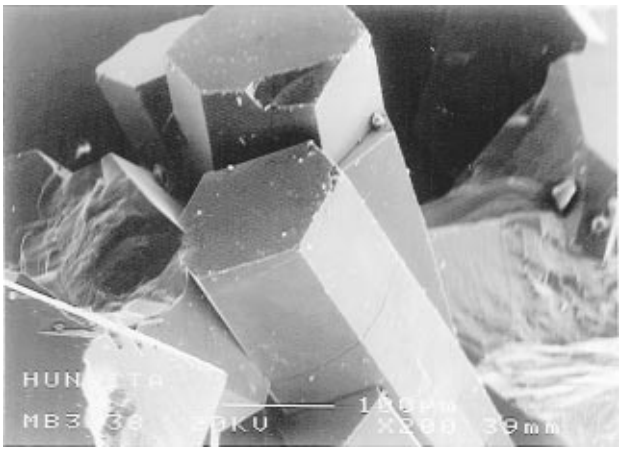

Figure 1. Crystals of $Fe_3La(BO_3)_4$ showing prismatic habit.

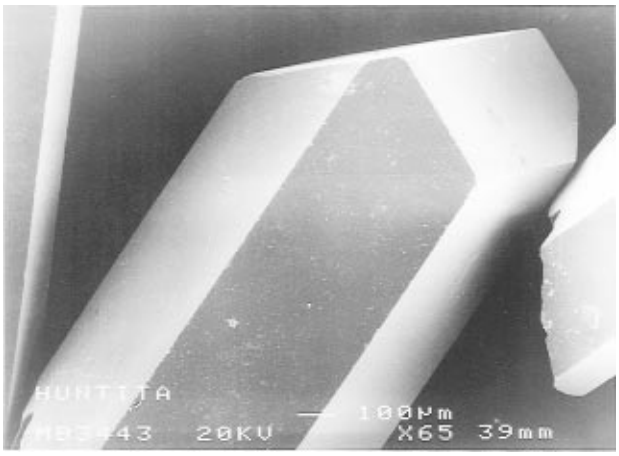

Figure 2. Rhombohedral crystals of $Fe_3Nd(BO_3)_4$ formed by hexagonal prisms combined with negative $(2\bar{1}\bar{1}1)$ rhombohedra.

Table 2. Atomic Positional Parameters and U_{eq} ($\times 10^3$) for $RFe_3(BO_3)_4$

atom	position	*x*	*y*	*z*	U_{eq}
R = La	3a	0	0	0	4(1)
Fe	9d	0.5515(1)	0	0	6(1)
B1	3b	0	0	1/2	12(2)
B2	9e	0.4470(9)	0	1/2	12(2)
O1	9e	0.8548(5)	0	1/2	9(1)
O2	9e	0.5881(7)	0	1/2	11(2)
O3	18f	0.4499(5)	0.1445(5)	0.5202(5)	12(1)
R = Nd	3a	0	0	0	4(1)
Fe	9d	0.5511(1)	0	0	3(1)
B1	3b	0	0	1/2	8(2)
B2	9e	0.4456(10)	0	1/2	7(2)
O1	9e	0.8557(6)	0	1/2	7(1)
O2	9e	0.5903(8)	0	1/2	10(2)
O3	18f	0.4511(6)	0.1453(6)	0.5188(6)	9(1)
R = Y, Bi[a]	3a	0	0	0	8(1)
Fe	9d	0.5505(2)	0	0	3(1)
B1	3b	0	0	1/2	9(3)
B2	9e	0.4495(15)	0	1/2	3(3)
O1	9e	0.8545(11)	0	1/2	6(2)
O2	9e	0.5934(11)	0	1/2	11(3)
O3	18f	0.4540(10)	0.1458(9)	0.5164(9)	9(3)

[a] Bi occupation factor at the Y site: 0.50(6).

(9) Walker, N.; Stuart, D. *Acta Crystallogr. A* **1983**, *39*, 158.
(10) Martínez-Ripoll, M.; Cano, F. H. *PESOS Program*; Instituto Rocasolano, CSIC, Madrid, 1975.
(11) Stewart, J. M.; Kundell, F. A.; Baldwin, J. C. *The X-Ray 80 System*; Computer Science Center, University of Maryland, College Park, MD, 1980.
(12) O'Connor, C. J. In *Progress in Inorganic Chemistry*; Lippard, S. K., Ed.; Wiley: New York, 1982; Vol. 29, p 210.

Table 3. Selected Bond Distances (Å) and Angles (deg) for $RFe_3(BO_3)_4$

R	La		Nd		$Y_{0.5}Bi_{0.5}$	
R−O(3)	2.420(4)	×6	2.403(4)	×6	2.372(6)	×6
Fe−O(1)	2.021(3)	×2	2.026(4)	×2	2.015(6)	×2
Fe−O(2)	2.055(5)	×2	2.044(5)	×2	2.026(7)	×2
Fe−O(3)	1.943(7)	×2	1.950(7)	×2	1.97(1)	×2
B1−O(1)	1.392(5)	×3	1.382(6)	×3	1.39(1)	×3
B2−O(2)	1.35(1)		1.39(1)		1.37(2)	
B2−O(3)	1.38(7)	×2	1.374(7)	×2	1.38(1)	×2
O(3)−R−O(3)	89.0(2)	×6	89.0(2)	×6	89.3(3)	×6
O(3)−R−O(3)	73.0(1)	×3	73.0(1)	×3	72.5(2)	×3
O(3)−R−O(3)	121.9(2)	×3	122.1(3)	×3	122.7(4)	×3
O(3)−R−O(3)	141.8(3)	×3	142.7(3)	×3	141.8(5)	×3
O(1)−Fe−O(2)	77.7(2)	×2	77.3(2)	×2	76.3(3)	×2
O(1)−Fe−O(1)	168.5(2)		168.5(2)		167.7(4)	
O(1)−Fe−O(2)	93.9(1)		94.4(1)		94.7(2)	
O(1)−Fe−O(3)	95.2(1)	×2	95.2(1)	×2	95.6(2)	×2
O(1)−Fe−O(3)	92.2(2)	×2	92.1(2)	×2	92.2(3)	×2
O(2)−Fe−O(1)	93.9(9)		94.4(2)		94.7(2)	
O(2)−Fe−O(2)	87.8(2)		87.8(2)		87.5(3)	
O(2)−Fe−O(3)	87.6(2)	×2	87.2(2)	×2	87.1(4)	×2
O(2)−Fe−O(3)	168.6(2)	×2	167.9(2)	×2	166.8(3)	×2
O(3)−Fe−O(3)	98.7(3)		99.6(3)		100.6(5)	
O(1)−B(1)−O(1)	120		120		120	
O(2)−B(2)−O(3)	118.8(3)	×2	117.9(4)	×2	118.3(6)	
O(3)−B(2)−O(3)	122.4(7)		124.2(8)		123(1)	

the crystal *c* axis. All the borate anions in the unit cell are distributed over three layers at $z/c = {}^1/_6$, $^1/_2$, and $^5/_6$. Each layer contains three B(2) and one B(1) borate anions. B(1)O_3 triangles are perpendicular to the *c* axis, and B(2)O_3 nearly so. The Fe cations are coordinated to three different types of oxygen atoms: O(1), from a B(1) borate anion at (3b); O(2) and O(3), both from B(2) borate anions at (9e). The R^{3+} cations, which are located between adjacent layers of anions, are coordinated to six O(3) atoms, three of them common to the B(2) borate anions of the layer above and the other three shared with B(2) borates of the layer below.

In tridimensional $Fe_3R(BO_3)_4$ the FeO_6 octahedra share edges in such a way that they form helicoidal chains which run parallel to the *c* axis and are mutually independent, as Figure 3 shows. In this 1D arrangement the Fe−Fe distances are relatively short: 3.178(2), 3.174(2), and 3.179(1) Å for R = Y, La, and Nd, respectively. RO_6 trigonal prisms are isolated polyhedra. Each of these RO_6 prisms connect three helicoidal chains of FeO_6 octahedra through common O(3) oxygen atoms and gives rise to R−Fe distances of 3.785(2), 3.7829(7), and 3.7719(7) Å for R = La, Nd, and Y, respectively. B(1)O_3 triangles share vertexes only with FeO_6 polyhedra. Each B(1)O_3 connects to three helicoidal chains of FeO_6 octahedra. Figure 4 illustrates the position of the B(1)O_3 triangles which lie above and below the RO_6 prisms and connect three helicoidal chains like RO_6 prisms do. B(1)O_3 triangles appear mutually eclipsed, and staggered to RO_6 trigonal prisms. Figure 4 also shows how B(1)O_3 triangles share two vertexes with two different chains of FeO_6 octahedra and the other with a RO_6 prism.

The structure of the $Fe_3R(BO_3)_4$ huntites can be viewed as formed by layers normal to the *c* axis (Figure 4) in which there are RO_6 trigonal prisms and smaller FeO_6 octahedra. RO_6 polyhedra are interconnected within the layers by corner sharing with BO_3 groups of two types and FeO_6 octahedra, but in such a way that each FeO_6 shares two edges, one from each neighboring layer. This edge-sharing forms, by three-FeO_6 octahedra-

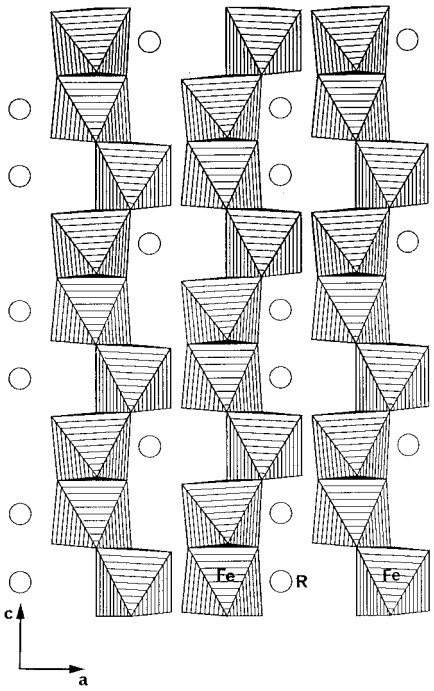

Figure 3. STRUPLO[13] view of the helicoidal chains of FeO_6 octahedra parallel to the *c* axis together with R atoms in $Fe_3R(BO_3)_4$.

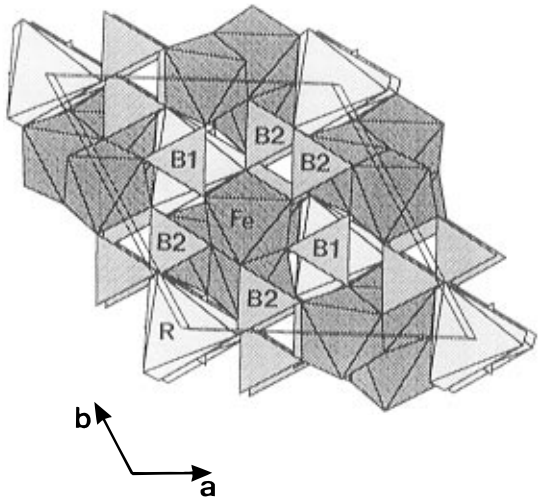

Figure 4. Projection on the *ab* plane of the $Fe_3R(BO_3)_4$ unit cell.

repeat, the infinite helicoidal chains running parallel to the *c* axis (Figure 3).

The temperature dependence of the molar magnetic susceptibility χ_m (and its reciprocal χ_m^{-1}) for $Fe_3R(BO_3)_4$, is shown in Figure 5 for R = Y, La, and Nd, respectively. Among the observed maxima in the χ_m curve at ≃260 K (255, 261, and 260 K) and ≃35 K (39.5, 32, and 32 K), for R = Y, La, and Nd, respectively, the most clearly observed were for Y^{3+} and La^{3+} materials, with no **f** electrons. In fact for R = Nd a very weak effect is seen at the highest temperature. On the other hand, at very low temperatures one clear and well-developed peak is observed at 6 K only for the Nd material (Figure 5c), although χ_m also shows a slight increase for both Y and La compounds (Figure 5a,b).

It seems plausible to attribute the magnetic interactions above 35 K to the occurrence of magnetic order within the Fe sublattice. The existence of a 1D ar-

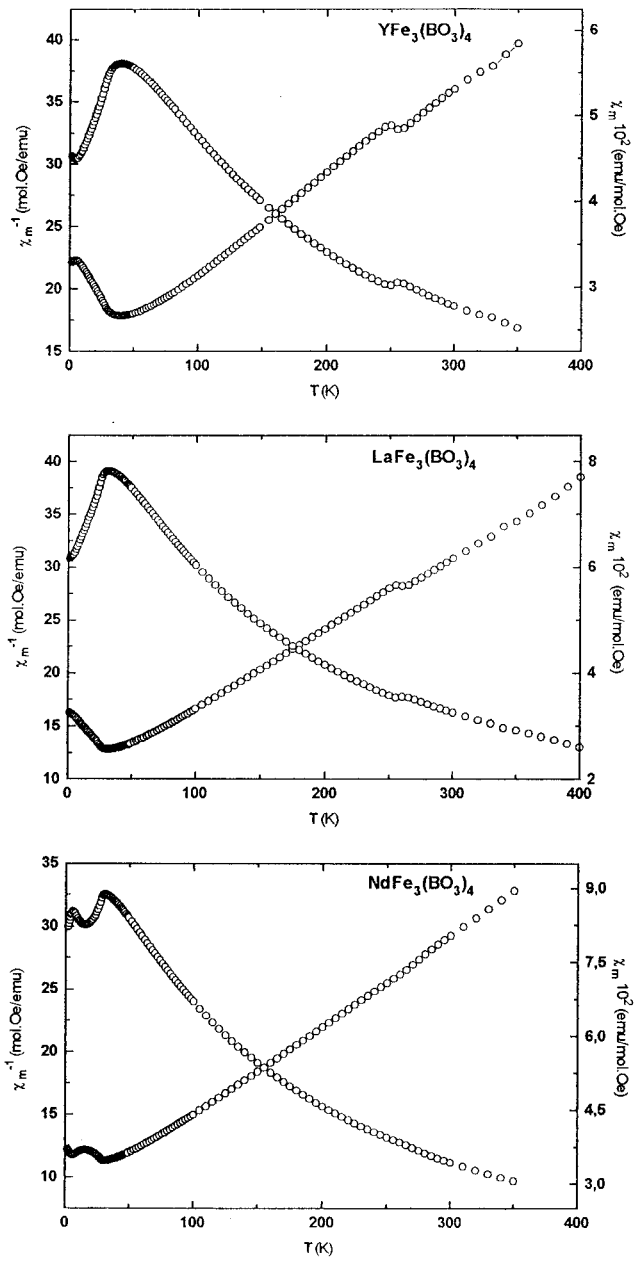

Figure 5. Molar magnetic susceptibility and its reciprocal as a function of temperature for (a, top) $Fe_3Y(BO_3)_4$, (b, middle) $Fe_3La(BO_3)_4$, and (c, bottom) $Fe_3Nd(BO_3)_4$.

rangement of edge sharing helicoidal chains of FeO_6 octahedra (Figure 3) with relatively short Fe−Fe distances, ≃3.18 Å, leads to superexchange Fe−Fe or Fe−O−Fe interactions. The net maximum found at 6 K for R = Nd can be related to a 3D antiferromagnetic ordering in both the Fe^{3+} and Nd^{3+} sublattices, where the most effective magnetic interactions probably occur in the Fe−O−Nd−O−Fe pathway, with angles of 120° ≪ 180° and large Fe−Fe distances between different chains that justify the low Néel temperature for this oxide. As was indicated, the RO_6 trigonal prisms are sharing corners with FeO_6 octahedra in the same layer and thus the existence of the maximum should strongly depend on the type of the rare-earth cation involved. The paramagnetic character of the R^{3+} cation seems to favor the long-distance interaction between the FeO_6 chains since these interactions do not exist so clearly for R = Y and La. This can confirm the above reasoning, similar to that previously proposed for other rare-earth 3d metal compounds.[14]

The $Fe_3R(BO_3)_4$ huntites can be compared with $FeBO_3$ and $NdBO_3$, which have the crystal structure of the two forms of $CaCO_3$, calcite and aragonite respectively. The iron borate is a canted antiferromagnet[15] with Curie temperature of 348 K and shows a small ferromagnetic moment at room temperature, and $NdBO_3$ is paramagnetic.[16] Like $NdBO_3$, $Fe_3Nd(BO_3)_4$ is paramagnetic from 70 K. In the range 70−350 K, its inverse magnetic susceptibility follows ($r = 0.9998$) the Curie law $\chi^{-1} = 7.85(3) + 0.0707(2)T$, with a Weiss temperature of −111.0 K and a molar magnetic moment of 10.61 μ_B, about one-half of the sum of the atomic moments. Both data suggest a pronounced antiferromagnetism. At lower temperatures the magnetic behavior of $Fe_3Nd(BO_3)_4$ is, like those of the Y and La compounds, quite different to those of the simple borates and is related to its own structural peculiarities as indicated.

The regular triangular coordination of boron in these compounds is confirmed by their infrared spectra. These show a broad group of bands at vibrational frequencies in the range 1400−1100 cm^{-1} which are due to the ν_d(B−O) stretching vibrations, whereas sharper bands at 775−650 cm^{-1} correspond to the $\pi(BO_3)$ modes, and those ranging between 600 and 500 cm^{-1} can be assigned to δ_d(O−B−O) bending modes.[17] Taking into account that B(2) has a less symmetrical triangular coordination, the small peaks observed at ≃1000 cm^{-1} can be attributed to ν_s(B−O) stretching vibrations that are IR-active for pyramidal symmetry. This last vibration is not clearly shown in the previous reported IR spectra of the Gd material.[4] Apart from ν_s all the remaining vibrations above 500 cm^{-1} are very similar to the corresponding modes in the IR spectra of rare-earth borates or 3d-metal borates with calcite structure and, obviously, to the spectrum of the huntite itself. Below 450 cm^{-1} the spectra are fairly complex. The strong vibrations observed would be attributed to ν(R−O) modes, whereas the lowest wavenumbers could be assigned to some (R−O) modes and bending vibrations of the RO_6 and FeO_6 polyhedra present in these materials.

Acknowledgment. This work was supported by the Spanish CICyT under Project No. PB94-0031. Magnetic measurements were performed by J. L. Martínez. The authors acknowledge the comments of J. González on the magnetic properties.

Supporting Information Available: Coefficients for the weighting scheme in $Fe_3R(BO_3)_4$ (R = La, Nd), anisotropic temperature factors for $Fe_3R(BO_3)_4$, and IR spectra of $FeR_3(BO_3)_4$ (R = Y, La, Nd) (3 pages); listings of structure factors for $Fe_3R(BO_3)_4$ (6 pages). Ordering information is given on any current masthead page.

CM960313M

(13) Fischer, R. X. *J. Appl. Crystallogr.* **1985**, *18*, 258.
(14) Hernández Velasco, J.; Sáez Puche, R. *J. Alloys Compd.* **1995**, *225*, 147.
(15) Wolfe, R.; Kurtzig, J.; LeCraw, R. C. *J. Appl. Phys.* **1970**, *41*, 1218.
(16) Antic-Fidancev, E.; Aride, J.; Chaminade, J.-P.; Lemaitre-Blaise, M.; Porcher, P. *J. Solid State Chem.* **1992**, *97*, 74.
(17) Nakamoto, K. *Infrared and Raman Spectra of Inorganic and Coordination Compounds*, 4th ed.; John Wiley: New York, 1986; pp 121−125, 476.